

# Context-Centric Target Localization with Optimal Anchor Deployments

Qingquan Zhang<sup>\*</sup>, Wei Xu<sup>†</sup>, Zhichuan Huang<sup>\*</sup>, Ziqiao Zhou<sup>‡</sup>, Ping Yi<sup>§</sup>, Ting Zhu<sup>\*</sup>, Sheng Xiao<sup>¶</sup>

<sup>\*</sup> University of Maryland, Baltimore County, USA

<sup>†</sup> University of North Carolina at Chapel Hill, USA

<sup>‡</sup> Northeastern University, USA

<sup>§</sup> Shanghai Jiao Tong University, China

<sup>¶</sup> Hunan University, China

**Abstract**—Localization proves to be a promising application of wireless sensor networks. Although a considerable number of algorithms have been designed for low-overhead and high-accuracy localization, problems remain to be tackled such as the way to use anchor-deploying. In this paper, we present a mechanism for range-free localization called Enhanced Map Segmentation (EMS) to deploy and segment the map where precise indoor localization is required. Despite the limits of environmental noise, sensing irregularity, received signal strength (RSS) variation and other unavoidable factors, EMS can be reliable by improving the quality of map segmentation. This paper will present and analyze the enhancing method by a series of simulations. In addition, to deal with ambiguous context positions that confounds the localization, this paper ameliorates the segmentation with context conception mentioned in [1] by statistical methods. In fact, a well-organized deployment and a context-based decision mechanism can make such a layer of abstraction more reliable and compatible.

## I. INTRODUCTION

Wireless sensor networks (WSNs) [2], [3] were proposed in the last century. Although no longer an emerging technology, they have been universally motivated by area surveillance applications [4], [5]. In contemporary society, there is not only the battlefield surveillance [6] but also the civil localization application implemented by WSNs where low-cost [3] sensor nodes are deployed randomly or deliberately. However, the absence of full-fledged localization strategy renders existing localization schemes far from optimal, which results in poor accuracy and enormous overheads [3].

In addition, the demand for higher accuracy, lower costs and shorter delays is on the rise as location-based mobile applications have emerged as the dominant paradigm. To keep up with the trend, some eminent ideas have been put forward to solve tracking with WSNs [7]–[9]. Traditionally, WSNs-based localization algorithms can be divided into two categories: range-free methods and range-based methods [10]. The latter is defined by protocols that use point-to-point distance estimates (range) or angle estimates for calculating location [11], [12], and the former makes no use of such information. Created with less range information, a range-free method, however, is more suitable for large-scale network localization applications, for the range-based one requires specific statistics and more expensive hardware or careful system calibration [10], [13], [14]. In addition, the range-free strategy has been extensively

studied in many algorithms such as the RSD [15], DV-Hop [16], APIT [17], and REP [18]. However, most of these algorithms ignore a less commonly recognized, but equally important factor, the spatial deployment of anchor nodes or base-stations in sensor networks, which is of great value to the robustness of localization schemes and other range-free methods.

The phenomenon unquestionably exists and has obvious significance for the vigorous efficiency of the sensor localization as well as for the accuracy of location estimations, statically and dynamically. Our work is also motivated by a serendipitous discovery that a simple assumption of random anchor node deployment can never provide an optimal solution in achieving desired accuracy in location estimations. For instance, it is hard in RSD for all of the node sequences to reach the maximum of possible permutation in the area with four or more Wireless Base Stations (called anchor(s) in the following description). This paper introduces the Enhanced Map Segmentation (EMS) in which the concept of segmentation is represented by division or partition in the following part and investigates an appropriate spatial deployment based on the following three assumptions: (i) The number of node sequences nearly equals to the number of subareas, and more subareas means more accuracy; (ii) The homogeneity [19], [20] of subdivisions, which can be analyzed by the area standard deviation, can decrease the location estimation errors; (iii) The relationship between application contexts and the subareas varies, thus context-based area segmentation and localization should be a practical consideration. The simulation and experiment results show that based on our area division strategy and context-based segmentation algorithm, the localization accuracy is significantly improved.

Based on our empirical study, the different deployments of anchor nodes make a significant impact on performance of range-free localization methods. Although numerous issues need solutions to achieve the optimal localization scheme, three fundamental challenges must first be addressed: the effective approach in area division, the dynamic characteristics of anchor node deployment, and the complexity of application contexts in network environments. It has long been known that existing range-free methods do not work in practice as they do in theory because they fail to extract an optimal

anchor node deployment scheme. However, through extensive simulations, we demonstrate that EMS is designed in line with our theoretical analysis and results in a better localization accuracy than other approaches with a random deployment assumption. Furthermore, we have tested significant batches of scenarios to validate our cogent EMS design. We also consider the existence of contexts in our analysis of optimal node deployment scheme. Thus our framework sheds light on the factors that dramatically increase the accuracy of location estimations.

The rest of the paper is organized as follows: Section II gives an overview about the design; Section III details the system design and discusses some practical promotions; Section IV evaluates the design with extensive simulations and makes several comparisons with other typical algorithms; Section V gives field experiments in real environments; Section VI briefly discusses related work; and Section VII concludes the paper.

## II. SYSTEM OVERVIEW

This section gives an overview of the EMS localization system. As shown in Fig. 1, the system consists of two critical components, i) map division, and ii) context-centric anchor deployment strategy in localization.

Without loss of generality, we start the discussion within a two-dimensional paradigm although our algorithm can be applied into a three-dimensional paradigm. In Fig. 1(a), four anchors have been deployed randomly. Once anchors are deployed, a topological graph is generated and the geometry relationship, such as their relative distances will be computed. Apparently, if different algorithms are used to define the relative distance, computed results, thus accuracy of location estimations, will be different. For example, the RSD is one of eminent state-in-art localization solutions that can approximately reduce 35% localization errors as compared with Sub-Hop resolutions [15]. In light of the EMS, let  $k$  be the number of anchors in a map, we define a high-dimensional location signature function as follows:

$$S(A) = (n_1, n_2, \dots, n_k) \quad (1)$$

where  $A$  is the subarea to which a target belongs,  $n_i$ ,  $1 \leq i \leq k$ , is the anchor number. The anchor sequence follows the relationship that  $RSS(n_i) > RSS(n_j)$  for all  $i < j$ . Similar to RSD, we can use the signature to mark all the positions in an area.

With perpendicular bisectors, an area can be divided into several subareas. As stated by Theorem 1, each subarea owns a unique high-dimensional location signature. Once a target gets into the area, as shown in Fig. 1(b), a signature will be generated and the relative distances to all the anchors, which are computed based on an algorithm that will be discussed later, can be achieved as well. As an example, the Fig. 1(b) shows that the signatures of a target  $T$ , anchor node  $A$  and anchor node  $B$  are rendered, and then used to get the relative distance between  $T$  and  $A$  and that between  $T$  and  $B$ . The flip theory used in RSD shows that the physical distance is in direct

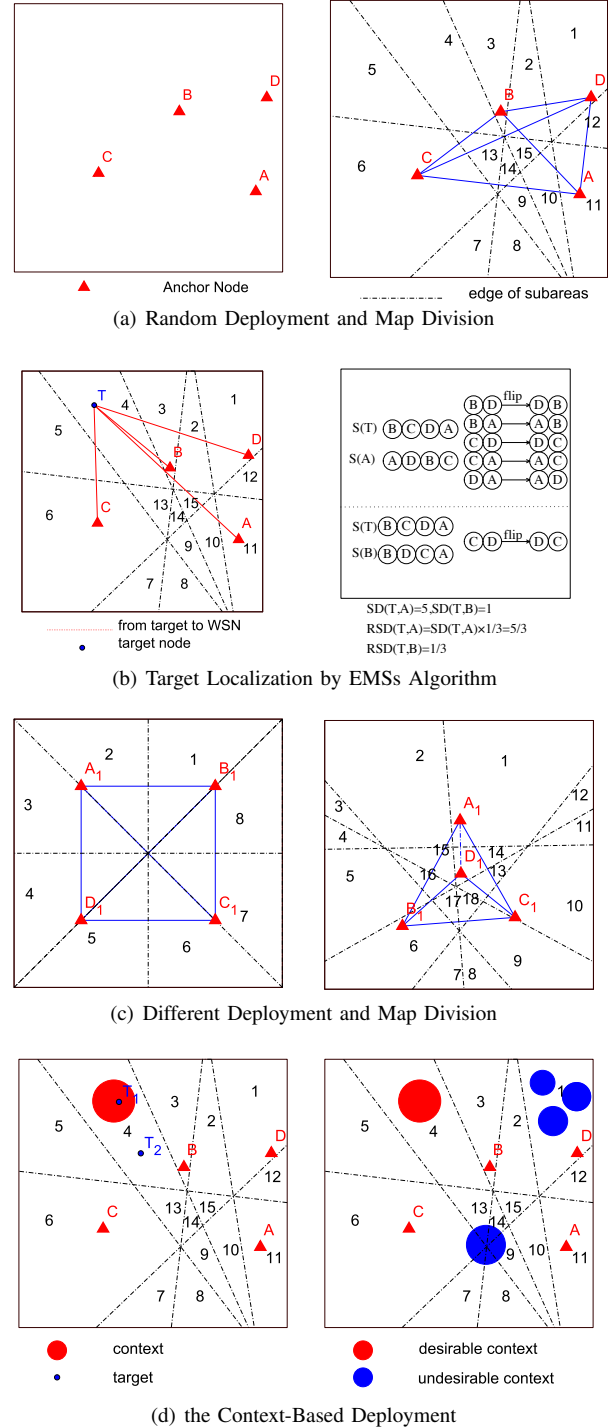


Fig. 1. Localization System Overview

proportion to the relative distances [15]. At this point, the target can be localized in one of the subareas and its location can then be estimated.

**Theorem 1.** *The signature function  $S$  defined in Equation 1 is bijective.*

*Proof:* Given a division of a map, let  $\mathbb{A}$  be the set of all subareas, and  $\mathbb{S}$  be the set of the signatures computed from  $\mathbb{A}$ . Clearly, both  $\mathbb{A}$  and  $\mathbb{S}$  are finite sets. The rest of this proof is done by contradiction.

Suppose  $S$  is not bijective, there will be only two possible suppositions : (i)  $\exists A_1, A_2 \in \mathbb{A} : A_1 \neq A_2 \wedge S(A_1) = S(A_2)$ , and (ii)  $\exists A \in \mathbb{A} \wedge \exists S_1(A), S_2(A) \in \mathbb{S} : S_1(A) \neq S_2(A)$ .

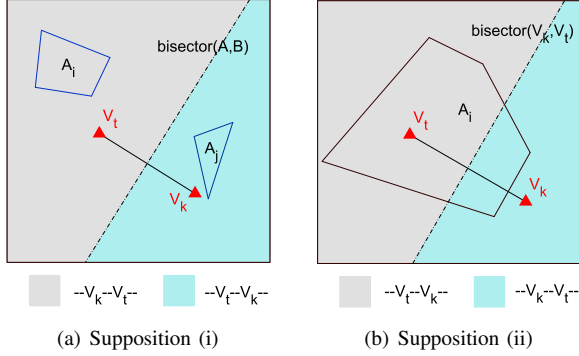


Fig. 2.  $S$  is Bijective

(i) As illustrated in Fig. 2(a), let  $A_i$  and  $A_j$  be two subareas divided by one or more bisectors, then there exists at least one bisector  $(V_k, V_t)$  so that  $A_i$  and  $A_j$  are located on different sides of  $(V_k, V_t)$ . If a target  $T$  has a signature  $S(A_i)$  in  $A_i$  initially, it will be impossible for  $T$  to hold an unchanged signature when it crosses the bisector  $(V_k, V_t)$  into the  $A_j$  because the relative position of  $V_k$  and  $V_t$  in the signature must flip.

(ii) As illustrated in Fig. 2(b), suppose a subarea  $A_i \in \mathbb{A}$  owns at least two different signatures  $S_1(A_i)$  and  $S_2(A_i)$ ,  $S_1(A_i) \neq S_2(A_i)$ , then there exists at least one flipped node pair, say,  $V_k$  and  $V_t$ . The bisector  $(V_k, V_t)$  must cross the  $A_i$ , which implies that  $A_i$  contains two subareas, contradicting the fact that  $A_i$  is *one* subarea.

In conclusion, the above two suppositions are both false, and thus  $S$  is bijective. ■

Based on Theorem 1, all the positions in the same subarea have the same signature. When a target enters an area, a signature is generated and the relative distances to all the anchors, which can be computed with an algorithm to be discussed later in this paper, can be obtained as well. Then the distances between the target of interest and the anchors can be computed with the definition in [15], and the physical distance is in direct proportion to the relative distances [15]. At this point, the target's location can be obtained.

In the above process, the deployment of those anchors is a determining factor. For instance, Fig. 1(c) provides one map with 8 subareas and another one with 18 subareas. The increase in the number of subareas, thus, can help to improve localization accuracy.

Meanwhile, the localization problem within contexts needs consideration in practice. We depict in Fig. 1(d) a few desirable or undesirable contexts. These contexts will degrade the performance of most existing localization schemes: either range-based or range-free, as neither of them assumes a perfect spatial environment. On the contrary, critical information is embedded in the contexts for localization problems, and we should make use of the relationship between contexts and

subareas to reduce overheads and to improve localization accuracy.

The rest of this paper will focus on the issues revealed in Fig. 1(c) and 1(d) to improve the accuracy of localization.

### III. SYSTEM DESIGN

In this section we present our system design from several aspects. We start with the ideal map division, and then introduce the map division with weight. Another two important topics – homogenization and context – are also discussed.

#### A. The Ideal Map Division

As mentioned earlier, a key task in management of localization is building technical solutions of anchor deployment to meet accuracy requirements. We capture this notion by means of area segmentation based on the positions of anchors. After all anchors deployed, the segmentation of region under surveillance can be determined by the fixed topological structure and the corresponding signatures.

Given the RSSs from available anchors, the physical information can be abstracted to the RSS signature in a region if the distribution of RSSs is known. The RSS distribution models have been well studied [21]–[23]. Because our EMS design by nature does not rely on the accuracy of RSSs, a simple relationship model that the RSS from an anchor is inverse proportion to the distance will suffice in our discussion.

To illustrate our concept, we start from a basic scenario in which there is no longer any communication barrier between any adjacent anchor pairs. Thus, a region, represented by a map, can be divided by the perpendicular bisectors between anchor pairs, and the geometry property of such a division will form our study foundation. Taking a map with two anchors,  $n_1$  and  $n_2$ , as an example, the bisector of  $n_1$  and  $n_2$  will divide the area into two subareas so that every point on one side of the bisector will see that its distance to anchor  $n_1$  will be smaller than that to anchor  $n_2$ , which implies that the RSS from anchor  $n_1$  will be stronger than that of  $n_2$  on any specific location in each sub-region. In this step, a relative signature [24] for any given point can be decided immediately by its relative location toward the bisector.

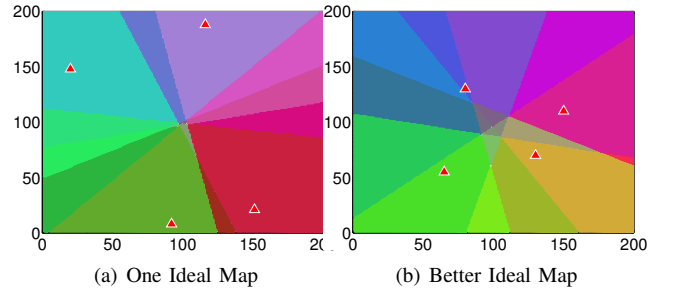


Fig. 3. Ideal Map

In this scenario, we evaluate the validity of ideal divisions. Without context constraints, the division of a map is determined by the number of anchors and their relative positions. Due to space limit, we will only present the results with 4 anchors setup, though experiments with a larger

number of anchors prove our proposition as well. It is worth mentioning that the example we showed in Fig. 3 is only two example of anchor deployments in which the maximum division, according to our maximum division proposition, can be achieved in the map. In other words, that shows how the maximum segmentation in our basic design is accessible. As shown in Fig. 3(a), subareas of different colors represent the respective signatures, which also indicates that the boundary is the straight line. Further simulations with different anchor deployment have been conducted, but the number of divisions in ideal map is 18 or less such as Fig. 3(b), which assures that our conclusion about the ultimate ideal division is self-evident.

### B. The Map Division with Weights

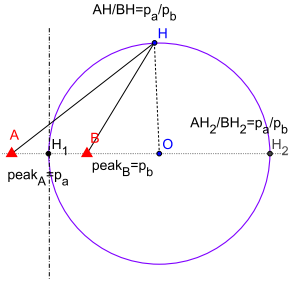


Fig. 4. Apollonius Circle

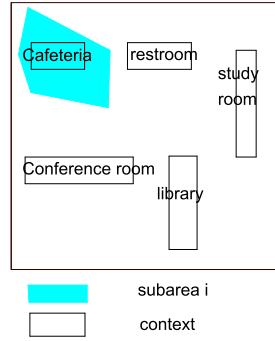


Fig. 5. A Map with Contexts

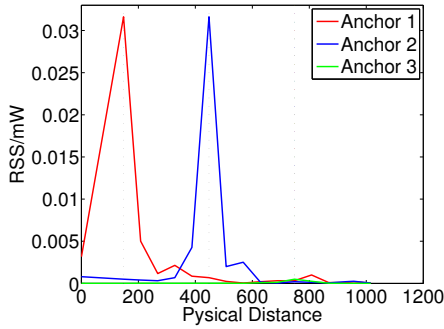


Fig. 6. A Field Result for Three Multiple Anchors

As mentioned in section III-A, we introduce the map division problem based on an ideal RSS distribution assumption in which all anchors are independent and identical. However, when it comes to a practical application, the vicious peak signals from different anchors as shown in Fig. III-B indicates the deflection of ideal case. The ideal map division ignores the fact that different anchors can either have peak signal strengths or their RSS distribution can be different due to spatial interference, which in turn will cause inaccurate location estimations. For further discussion, we define the following concepts:

**Definition 1.** The weight of an anchor node  $n$ , denoted  $W(n)$ , is  $W(n) \equiv 1/RSS_{peak}(n)$ , where  $RSS_{peak}(n)$  is the peak RSS from  $n$ .

**Definition 2.** The Distance with Weight between a target  $T$  and an anchor  $n$ , denoted  $DW(T, n)$ , is the product of the geometric distance between  $T$  and  $n$  and  $W(n)$ .

We use  $RSS_{peak}(n)$  to denote the peak RSS of an anchor  $n$ ; and when we are not interested in which anchor  $n$  is of interested, we simply use  $RSS_{peak}$  to refer to the peak RSS of an arbitrary anchor. In the next discussion, we use the RSS model defined in [25] as follows:

$$RSS = \frac{RSS_{peak}}{\left(\frac{r_u}{r_0}\right)^m} \cdot k \quad (2)$$

where,  $k$  and  $m$  are constant factors, and  $r_0$  is a reference distance in our model.

The optimal location estimation, therefore, depends on the accuracy of the peak value in our folder. Assuming the  $RSS_{peak}$  follows a normal distribution, i.e.,  $RSS_{peak} \sim N(\mu_0, \sigma_0^2)$ , there have been prior beliefs about the  $E(RSS_{peak}) = \mu_0$ , and  $\sigma(RSS_{peak}) = \sigma_0$ ,  $\mu_0$  and  $\sigma_0$  represent the best guess for  $RSS_{peak}$  and the uncertainty on the guess, which come from our prior experiments or specification of service provider. Thus, we need to modify the inputs to Equation 2 based on the in-situ estimation of  $\hat{RSS}_{peak}$  and  $\hat{\sigma}(RSS_{peak})$  [26]. The standard estimator of the expectations in this context is the sample mean

$$\hat{\mu} = \frac{1}{k} \sum_{t=1}^k X_T \sim N\left(\mu_1, \frac{\sigma_1^2}{k}\right) \quad (3)$$

where  $k$  is the number of the available sampling series. The sample mean is a highly inefficient estimator as the sampling estimation varies wildly when different sampling series are fed into the estimation process [26]. One way to cope with this issue is to use a more efficient *balance* estimator:

$$\mu^{(b)} \equiv (1 - b)\hat{\mu} + b\pi^0 \quad (4)$$

where  $\pi^0$  is our best guess,  $\pi^0 \sim N(\mu_0, \sigma_0^2)$  and  $0 \leq b \leq 1$  is the balance factor. The purpose is then to minimize balance  $\sigma_b$  under any given  $\mu^{(b)}$ . We can formalize our model as

$$\begin{aligned} & \text{Minimize } \sigma_b^2 = b'Vb \\ & \text{Subject to } E(\mu_0) = b'U = \bar{\mu} \\ & \sum_{i=1}^n b_i = 1 \end{aligned} \quad (5)$$

where  $V$  is covariance matrix between  $\hat{\mu}$  and  $\pi^0$ , and  $U$  is the vector  $[\mu_0, \mu_1]$ . The first solution to this formula is

$$Vb = \lambda U, \rightarrow b = \lambda V^{-1}U$$

Thus, the optimal balance factors given by the answer are used to derive the  $u^{(b)}$ , which in turn, is put into Equation 2.

Assuming that an anchor's  $RSS_{peak}$  is symmetric at all directions,  $RSS_{peak}$  defines a circle. After anchors with different  $RSS_{peak}$  are deployed, the division boundaries will become arcs rather than straight lines. And the new boundary curve is a Apollonius circle [27], as illustrated in Fig. 4. And

based on the modification, the map division with weight is created as described in Algorithm 1. Note that the total number of divisions made by weight-based approach can be larger than that by straight lines used in an ideal map division. The following Lemma 1 gives the maximum number of subareas that can be made under the weight-based division algorithm.

**Lemma 1.** *Given a map and  $m$  circles, the maximum number, denoted  $f(m)$ , of subareas into which could be divided by the  $m$  circles is given by*

$$f(m) = m^2 - m + 2 \quad (6)$$

*Proof:* The Equation 6 can be proved by induction. Obviously, One circle only divide the plain into two part. If there are  $m$  circles, at most  $2m$  points of intersection can be generated once one more circle join the plain, which will divide the circles into  $2m$  arcs. Each arc can divide one old subarea into 2 part, so that there can be at most  $2m$  additional parts. So the we can get the induction as following:

$$\left. \begin{aligned} f(1) &= 2 \\ f(k+1) - f(k) &= 2k, k = 1, 2, \dots, m-1 \end{aligned} \right\} \Rightarrow$$

$$f(m) = 2 + \sum_{k=1}^{m-1} 2k = m^2 - m + 2 \quad (7)$$

This finishes the proof. ■

**Corollary 1.** *Given a division of a map, there are at most  $f(m) = m^2 - m + 2$  different signatures.*

*Proof:* This corollary immediately follows Theorem 1 and Lemma 1. ■

As Equation 6 suggests, the maximum number of divisions is  $6^2 - 6 + 2 = 32$ , which conflicts with our former analysis with straight lines. As such, it is reasonable to analyze the facets of the dynamics of map division manner on which the circles will have impacts. On the one hand, the sequence permutation in signatures can easily illustrate that the maximum partition can not be beyond  $N_s!$  and  $f(\binom{N_s}{2})$  in the weight-based division, where  $N_s$  is the total number of available anchors deployed. On other hand, it is similar to the ideal map division in that the boundaries are not unlimited but limited by anchors (Specificly, such limitation will reduce  $\binom{N_s}{3} \cdot 2$  subareas after analyzing the graph theory).

According to our theory and simulation, the maximum number of divisions is apparently improved in a map with weight, compared with the ideal map. In a map with four anchors, for instance, the weight-based map can locate 24 subareas, higher than 18 subareas that ideal division can generate. This actually offer more flexibility in localization planning.

Note that, the maximum number of divisions (and thus the maximum number of signatures) is achieved only under certain anchor deployments. In Fig. 7, we fix the positions for three anchors  $n_1, n_2, n_3$  and move Anchor  $n_4$  in the scenario with a specific weight. After thousands of trial runs in Algorithm 1, we found out that not every kind of anchor deployments can get a maximum division, 24 parts in this case, as shown in

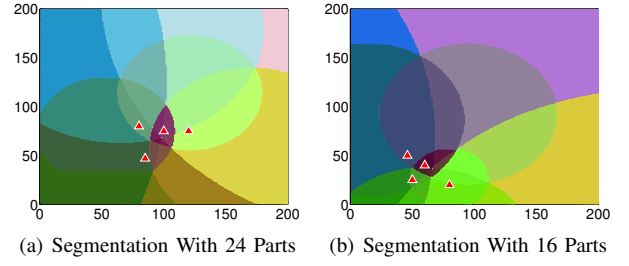


Fig. 7. Map Division with Weight

---

#### Algorithm 1 Map Division with Weight

---

**Require:** set the  $RSS_{peak}$  of the anchor  $i$ ,  $point \leftarrow (0, 0)$   
distance between point and anchor  $i$ ,  $rss_i \leftarrow$  the received  
 $RSS$  from anchor  $i$

**Ensure:**  $u^{(b)}$ , generate all the possible *signatures* of subareas

- 1: **while** the point still scanning the map **do**
  - 2:   **for**  $i \leftarrow 1$  to 4 **do**
  - 3:      $rss_i \leftarrow$  output from Equ 2;
  - 4:   **end for**
  - 5:    $sequence \leftarrow$  sort the  $RSSs$ ;
  - 6:    $signature(x, y) \leftarrow$  the anchor sequence in  $sequence$ ;
  - 7:   point moves to the next;
  - 8: **end while**
  - 9: generate the fixed map with different signatures;
- 

Fig. 7(a) and Fig. 7(b). When anchor 1, 2 and 3 are placed at positions such as (40, 120), (80, 120), and (160, 120), the maximum number of total divisions is only 16; but when placed at positions (80, 16), (48, 24), (36, 48), it can reach to 24.

#### C. The Effect of Homogenization

Although the number of map divisions in practice can reach the theoretical maximums, for example, 18 divisions in Fig. 3(a) or 24 divisions in Fig. 7(b), some subareas are so small (large) that no context (or multiple contexts) will be located in those subareas. Such division heterogeneity can lead to location estimation errors which can, however, be reduced through careful consideration. Next we evaluate the impact of division heterogeneity and attempt to capture the homogenization of map divisions. The homogeneity of divisions refers to the degree to which the sizes of all divisions are similar. And what we need to consider is how to quantify the division homogeneity. Although there are many effective algorithms we can choose to measure the homogenization, we should remember, however, that the goal here is not to achieve the division homogenization but to validate whether it can help to reduce location estimation errors [28]. To simplify the problem, we choose the standard deviation of division areas as a metric in our model. Then we adopt similar traversing techniques as we did in previous section to conduct experiments.

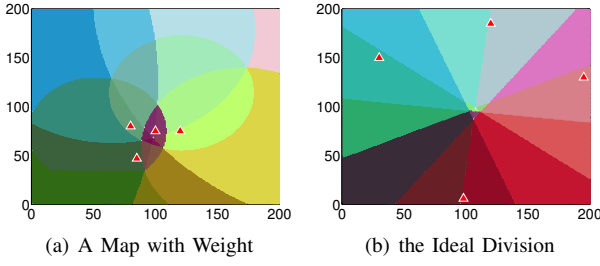


Fig. 8. Optimal Division of a Map

In this experiment, we have tested extensively all kinds of deployment schemes for 4 anchors. One typical result is shown in Fig. 8, which indicates that the optimal deployments of ideal or weighed divisions are so different from the one in the random scheme. However, even as the division standard deviation approaches to the minimum from our samples, not all of those subareas based on our optimal division scheme seem to share similar shapes. In a sense, this represents that deployment by ignoring the contexts may overstate statistical optimizer used in our experiments. In the next experiment, we will concentrate on the context-based scenario.

#### D. The Impact of Contexts in Map Division

In real-world localization applications, we need to track targets in application environments with which the practical contexts, for example, a study room on a campus building or a restaurant in a shopping mall, are associated. Generally speaking, when containing these contexts, the environment usually shows up as many targets gathering within these contexts. Thus, instead of ignoring those contexts as many existing algorithms do, we take the context factor into account when applying our EMS to address the localization problem (termed EMS-C in the rest of this paper). Clearly the contexts are linked to social activities or spatial constraints. To estimate the user behavior in these contexts, the probability model is used, which can be summarized and improved with practical localization data gathering. Therefore, two different models corresponding to those factors are brought into our design: (i) applying the probabilities sampled from a series of random simulation or derived from practical experiments to the subarea in order to decrease the errors on the division boundary; and (ii) deploying the anchors based on the context positions so that the context can own a unique signature so that the location estimation errors that vary from place to place can be reduced. To illustrate these two ideas, a map with contexts is shown as Fig. 5. The probability ( $p_c$ ) used in the subarea represents the probability of a target's presence in cafe when randomly moving into the subarea  $i$  ( $A_i$ ).

Although EMS-C can use the signature to judge which subarea a specific position belongs to, it is hard to estimate the deviation from the real position without further information processing. In order to indicate the signature of a specific subarea from the position perspective, we define the signature position ( $x, y$ ) of the subarea:

$$(x, y) = \frac{\sum (x, y)_c \cdot p_c}{pointSum_c} + \frac{\sum (x, y)_{nc} \cdot (1 - p_c)}{pointSum_{nc}} \quad (8)$$

where  $(x, y)_c \in context$ ,  $(x, y)_{nc} \notin context$ . In other words, every position with the same context signature is estimated to locate at  $(x, y)$  in Equation 8.

While applying EMS-C in practice, two issues needs consideration, as described below:

**Multi-Context Mistakes.** When two or more contexts locate completely or partially in one subarea, which context the target is in will not affect the signature so that the localizer cannot differentiate these two parts.

**Waste of Signature.** If a context occupies two or more subareas, two or more signatures will represent only one context. This will result in inefficient use of signatures. If a redundant signature is distributed to other contexts, the localization needs further elaboration to specify more context positions. Therefore, if some contexts own more than two signatures, the same localization precision can be achieved with fewer signatures or fewer anchors so that each context owns a unique signature.

The above observations form our motivation to discover a context-centric anchor deployment in the EMS-C.

In the rest of this section, we will answer the questions brought forward at the beginning of this paper: (i) what factors drive the complexity of context-based situation? (ii) what outcomes can be expected from such an analysis, the suitable deployment or the optimal deployment?

- *The suitable deployment.* This deployment is a match for the context, in which every context locates in different subarea and owns an unique signature.
- *The optimal deployment.* This deployment is a special suitable deployment, which has a minimum standard deviation of all subareas as well as the maximum number of partitions.

As implied in the preceding discussion, the optimal deployment, from a practical perspective, will underpin the accuracy of location estimations. Hence, the findings of all possible suitable deployment schemes is a key element characterizing this stage. The decision process that leads us to pursue a aggressive scanning technique involves four basic steps: (i) traverse deployments; (ii) compute the signatures and segment the map (iii) select the suitable deployment; (iv) find optimal deployment among different suitable deployments.

We demonstrate the results with the following examples. And two particular factors, the quantity of contexts and their respective area of influence usually conveyed by applications, are our major concerns. In the Fig. 9, we demonstrate two sets of experiments that have been conducted in our examples. One set is to study the effects due to the quantity variation of the contexts, described as rectangle areas in the Figure. The other is to compare the influence that contexts do to two map division schemes. From Fig. 9(a) and Fig. 9(c), we can tell clearly that when the number of contexts increases more or the contexts become more diverse, the complexity of achieving the optimal deployment scheme will become much higher due to the heterogeneity of contexts. Similar results can be found in the weight-based division scheme as shown in Fig. 9(b) and Fig. 9(d).

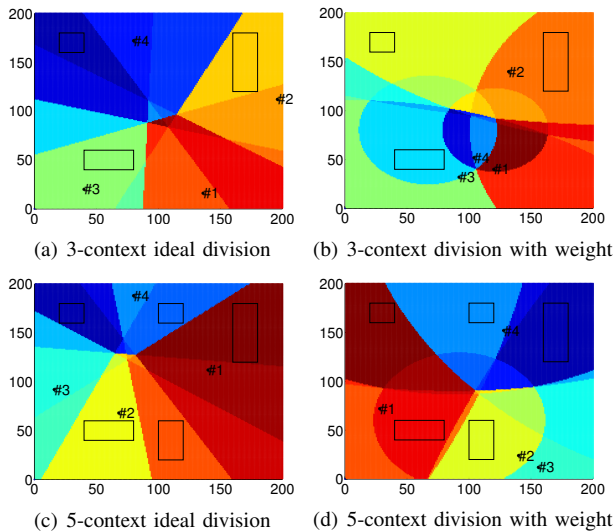


Fig. 9. Best Context-Based Division of Map

To tackle these challenges, some heuristic approaches will be applied in our model, like refining the traversal algorithm or exploiting the changing regulation of parameter-standard deviation and number of partitions as specified in the definition of “optimal deployment”.

#### IV. SYSTEM EVALUATION BY COMPARISON

This section gives intuitive discussions about the merits of the EMS in comparison with one popular algorithms (RSSI), and the improvement effects from EMS to EMS-C. From the perspectives of accuracy and error rate, a satisfying conclusion about EMS is reached by several statistical graphs.

##### A. Evaluation Criteria

Before the simulation, we summarize the evaluation criterion for localization. When saying a localization method is better, we usually emphasize that the computed position is more approximate to the real position. So we can use the difference between the real position and estimated position as the criteria to show the performance of our localization algorithm, which we call as Error Distance (ED).

##### B. RSSI VS EMS

This section compares Received Signal Strength Indication (RSSI), a universal method for localization, which makes the most of the method of trilateration, with our proposed EMS method. RSSI needs three RSS values from three anchors and the initial information of anchor positions to compute the location of a target by trilateration.

Similar to other researchers, we also use average error distances (the unit of error distance here is represented as base unit of the gridding system in our simulation); that is, the distance deviation between the projected location and the ground true position, as one of our metrics. To evaluate the error distance, a simulation is designed to compare the deviations between the factual positions and the computed positions by the two methods: the RSSI and EMS. In this section, we plant an increasing number of anchors,  $n$ , from

five to eight, to make an error comparison between them. In our experiments, an estimated signal peak value, which is set to be lower than each anchor’s *PeakValue*, is used for the computed distance between the point and the anchors. Moreover, to provide a better understanding between the RSSI and EMS, we study the location estimation performance of two methods by investigating their respective localization errors under different distances to our reference points, e.g., anchor nodes with known positions. We pick up the points which have relative distances  $r$ , ranging from 1 to 40, to a reference anchor as testing samples.

We will illustrate our discoveries by using one typical example of our experiments. At the beginning, there are five anchors in the map, which can divide the whole area into 40 parts, as shown in Fig. 10(a). Then, after conducting the simulation and picking up the points at  $r$  (from 1 to 40) to the referenced anchor, we finally get the results shown in Fig. 11(a). As we extend the simulations, more anchors are introduced and the corresponding division results are achieved and shown in Fig. 10. As complements for the Fig. 11(a), the extensive results tend to be more effective, which can be seen in Fig. 11(b), 11(c) and 11(d).

Based on the results, we can see that EMS demonstrates smaller error rates than RSSI in most of the situations. In addition, with more anchors introduced, a higher accuracy and lower error rate in localization can be achieved, as shown in Fig. 12. For example, in Fig. 11(c), the average error distance is about nine, compared to the average 17 in Fig. 11(a). With further analysis, we find that the error variation in Fig. 11(a) results from uneven divisions, which can be improved by better anchor deployments or context constraints.

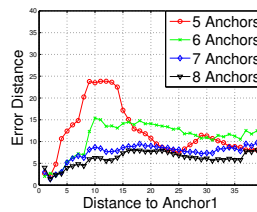


Fig. 12. Deviation Evaluation with Multiple of Anchors

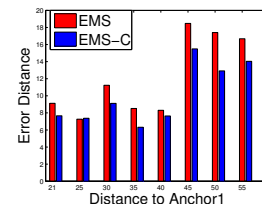


Fig. 13. Deviation Evaluation Between EMS and EMS-C

##### C. EMS VS EMS-C

We compare EMS and EMS-C in this section, adding some 10-radius circles as contexts into the subareas of the map with five anchors. In the simulation of this part, point moves randomly in the map except on the boundary of a context, on which it enters the context with a fixed probability,  $P_c$ . After conducting the simulation in the same configuration as that in sectionIV-B, we can get the  $EDs$  of the points at all the positions in the area. Because it’s hard to add contexts into the very small subareas on the central part of the map, as shown in Fig. 10(a), it doesn’t make sense if we pick up the points in these subareas, so we choose only the points at the distance  $r$ , ranging from 20 to 55 to the reference anchor,

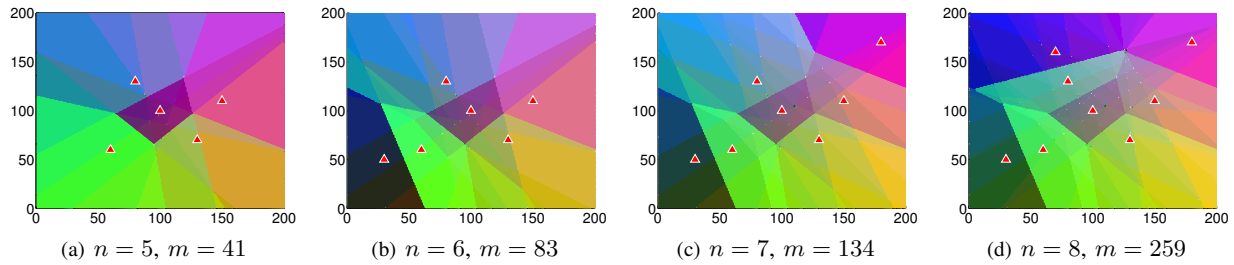
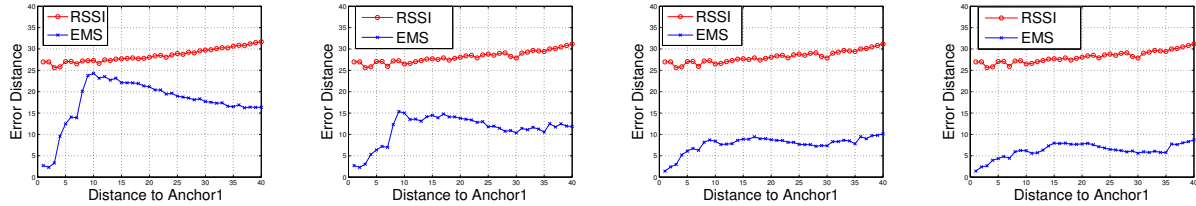


Fig. 10. EMS Divisions with  $n$  anchors and  $m$  subareas



(a) RSSI VS EMS with 5 anchors (b) RSSI VS EMS with 6 anchors (c) RSSI VS EMS with 7 anchors (d) RSSI VS EMS with 8 anchors

Fig. 11. Deviation Evaluation Between EMS and RSSI

and finally we can generate the result shown in Fig. 13. The figure intuitively depicts that EMS-C can observably lower the deviation of EMS, which informs us that adding contexts into subareas can improve the accuracy of locating.

#### D. Comparison with Some Advanced or Classical Algorithm

Finally, the results of our experiments are compared with other advanced and classical algorithms such as EZ, Unloc, and DV-hop. We show the results in Table I.

Name	EZ	Unloc	DV-hop	EMS
Accuracy	2-7m	2-7m	5-10m	2-4m
Pitfalls	GPS Lock	intensive prior study	considerable error distance	anchor deployment sensitive

TABLE I  
COMPARISON AMONG FOUR ALGORITHMS

Based on our experiments, the proposed EMS and EMS-C outperform unLoc and EZ under few anchor conditions, and require no additional prior field study. It can be highly expected that increasing the number of anchors can further enhance the system performance.

#### V. TEST-BED EXPERIMENTATION



Fig. 14. The wireless hotspot

In this section, we report field experiments with wireless anchors. To be more specific, we conducted experiments in environments such as i) an office environment, and ii) a gym and ii) student apartments. The interference can vary significantly in these three places. The first two sets of experiments were settled in ideal environments. The third sets of experiments, on the other hand, were conducted in a rather complex condition, with concrete walls and other surroundings. An android-based Samsung Galaxy SIII smartphone, powered with WiFi HT40 radio, is used as a mobile platform. Our self-developed app which can scan the RF signals and Wi-Fi signals is installed onto the smartphone to detect the RSSs from our wireless anchors. The app can communicate with our center platform where the data will be processed and EFD algorithm will be conducted. A self-designed wireless hotspots powered by a broad-band omnidirectional monopole antenna with 16DB gain are used as the wireless anchors, as shown in Fig. 14. A detailed descriptions of these experiments in detail are presented as follows.

#### A. Data Processing and Evaluation Criterion

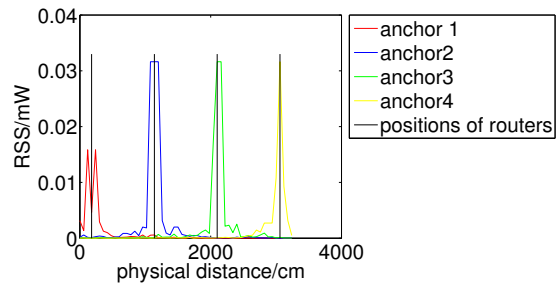


Fig. 15. Fitted Curve by Sampling Data Set

In this experiment, RSS values and position information of the moving android device were collected after the prior RSS

values and the anchors' positions were measured. They will be divided into two sets: (i) One set is the calibration data, including four anchors' positions and several RSS values from four anchors at a small set of locations, which were used to adjust parameters, such as the peak values, used by the EMS algorithm; (ii) Another set is the sampling data set, as shown in Fig. 15, including a much larger scale of RSS values from four anchors measured at various positions, which were used to evaluate our system. In data processing, we use ED to evaluate the localization performance.

### B. Experiments in Friendly Environments

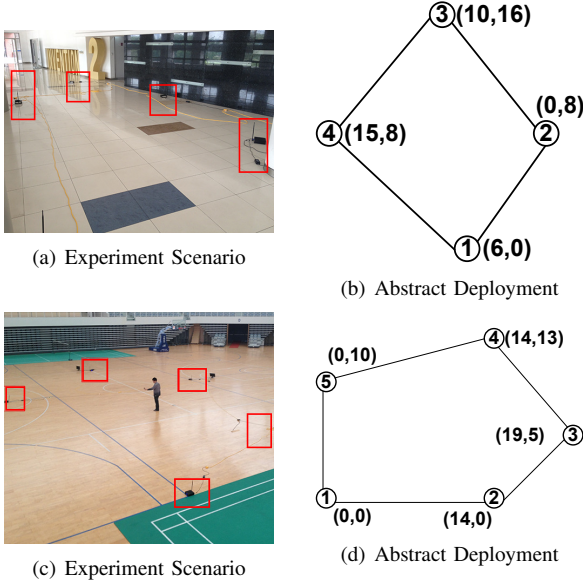


Fig. 16. Experiments in Friendly Environments

First, we intended to quantify the performance of the EMS in an office environment. In the Engineering building of Shanghai Jiaotong University, as shown in Fig. 16(a), four anchors are set according to the algorithms described, their positions can be viewed in Fig. 16(b). We walked randomly along the hallway with a mean of 1 meter/second, and measured the localization errors at different spots. The EMS system demonstrated an average error distance of 1.41 meter. Besides, to further test the complexity of our system, we also set five anchors in a stadium, as shown in Fig. 16(c). Similarly, we randomly walked around on the field with normal velocity of the pedestrian. The average error distances of these experiments is 1.9 meter.

### C. Results in Student Apartments

To test our mechanism in an environment with fierce interference, we placed anchors in four different student apartments. Two optimal deployment schemes have been selected in our experiments. The configuration of the first anchor deployment is shown in Fig. 17(a). Typically, concrete walls and surroundings can cause serious performance degradation due to RF fading and multipaths effects. However, we find that the localization system correctly captured the signatures for all the experimental points and the average error distance of

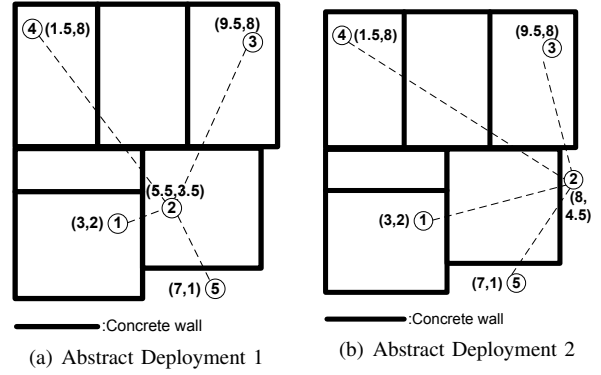


Fig. 17. Experiments in Student Apartments

these experiments is 2.09meter. In the second scheme, another optimal anchor deployment was used, as shown in Fig. 17(b). The measured average localization error is 2.18meter.

## VI. RELATED WORK

Localization in sensor networks has been an active research topic recently [29]–[33]. Due to space constraints, we can mention only a few directly related works here.

Two recent works about the algorithm, RSD [15] and RND [20], are novel range-free algorithms for localization. Both methods lay stress on the complicated formula used to compute a relative distance which is used to get the position by the trilateration. Although the trilateration is indeed a remarkable universal method in tracking, the different models based on the trilateration result in different modifying factors; for instance, the Regulated Signature Distance (RSD) is the extension for Signature Distance (SD) with a regulated modifying factor, considering the heterogeneous. The long-term research and practice do not significantly ameliorate the result, which, on the contrary, often leads into the stubborn insistence of a complicated equation for relative distance. On the other hand, both methods focus less on the practical scenario and understate the influence of different deployment. In both algorithms, the peak signal strength has never been considered, and the circle-shaped border has never been used to segment the field; instead they treat the peak signal as the same and borders as straight lines. This paper differs from them significantly by (i) replacing the trilateration with map segmentation method, (ii) bringing in the context concept for practical location, and (iii) testing our simulation with different deployments and alterable anchors, rather than only with several fixed deployment configurations.

## VII. CONCLUSION

This paper presents a range-free localization method called EMS, which promotes the precision with less costs and emphasizes the effect of anchors and contexts, on the practical deployment. Tracking is modeled as a signature matching problem in our design. Besides the basic design of the EMS method, some heuristic approaches, to be specific, the weight-based approach and the context-based location estimation technique, are proposed to enhance the system performance.

In addition, the design provides thorough analysis on several practical scenarios in which relatively optimal anchor deployment schemes are derived. Based on the current features of this mechanism, such as easy-to-deploy and area-division-based, it can be widely implemented in scenarios like localizing in indoor emergencies and in-door customer behaviour analyses. The detailed analytical evaluation demonstrates that the EMS method provides a higher-accuracy and fewer-error strategy for localization than the universal trilateration method. Simulations show that our EMS can reduce error distance by 37.8% when we segment the map with five anchors, 63.7% with six anchors, 72.6% with seven anchors, 78.0% with eight anchors, and higher rate with more anchors, and that EMS-C, compared to EMS, can reduce the error distance by 13.73% in a five anchors map. Furthermore, our experimental results also validate the effectiveness of our EMS method and demonstrate a better performance than other range-free approaches. In the future, we intend to enhance the localization system performance by investigating the interference from different surroundings and contexts, which we believe will further reduce the design complexity and increase localization accuracy.

#### ACKNOWLEDGE

This work is supported by NSF CNS-1503590 and CNS-1539047.

#### REFERENCES

- [1] Y. Liu, S. Lu, and Y. Liu, "Coal: Context aware localization for high energy efficiency in wireless networks," in *Wireless Communications and Networking Conference (WCNC), 2011 IEEE*. IEEE, 2011, pp. 2030–2035.
- [2] M. Rudafshani and S. Datta, "Localization in wireless sensor networks," in *Information Processing in Sensor Networks, 2007. IPSN 2007. 6th International Symposium on*. IEEE, 2007, pp. 51–60.
- [3] A. Pal, "Localization algorithms in wireless sensor networks: Current approaches and future challenges," *Network Protocols and Algorithms*, vol. 2, no. 1, pp. 45–73, 2010.
- [4] J. Hicks, A. Christian, and B. Avery, "Integrating presence and location services using sip," *HP TechCon*, 2004.
- [5] A. Terzis, A. Anandarajah, K. Moore, I. Wang *et al.*, "Slip surface localization in wireless sensor networks for landslide prediction," in *Proceedings of the 5th international conference on Information processing in sensor networks*. ACM, 2006, pp. 109–116.
- [6] T. Bokareva, W. Hu, S. Kanhere, B. Ristic, N. Gordon, T. Bessell, M. Rutten, and S. Jha, "Wireless sensor networks for battlefield surveillance," in *Proceedings of the land warfare conference*, 2006.
- [7] N. Patwari, J. N. Ash, S. Kyperountas, A. O. Hero, R. L. Moses, and N. S. Correal, "Locating the nodes: cooperative localization in wireless sensor networks," *Signal Processing Magazine, IEEE*, vol. 22, no. 4, pp. 54–69, 2005.
- [8] A. Vempaty, O. Ozdemir, K. Agrawal, H. Chen, and P. K. Varshney, "Localization in wireless sensor networks: Byzantines and mitigation techniques," *Signal Processing, IEEE Transactions on*, vol. 61, no. 6, pp. 1495–1508, 2013.
- [9] J. W. Branch, C. Giannella, B. Szymanski, R. Wolff, and H. Kargupta, "In-network outlier detection in wireless sensor networks," *Knowledge and information systems*, vol. 34, no. 1, pp. 23–54, 2013.
- [10] X. Luo, Y. Liu, C. Long, and J. Luo, "Range-free localization algorithms in wireless sensor networks," in *Fifth International Conference on Machine Vision (ICMV 12)*. International Society for Optics and Photonics, 2013, pp. 87 842A–87 842A.
- [11] S. Zhang, J. Cao, C. Li-Jun, and D. Chen, "Accurate and energy-efficient range-free localization for mobile sensor networks," *Mobile Computing, IEEE Transactions on*, vol. 9, no. 6, pp. 897–910, 2010.
- [12] A. Boukerche, H. Oliveira, E. F. Nakamura, and A. A. Loureiro, "Localization systems for wireless sensor networks," *wireless Communications, IEEE*, vol. 14, no. 6, pp. 6–12, 2007.
- [13] D. Niculescu and B. Nath, "Ad hoc positioning system (aps) using aoa," in *INFOCOM 2003. Twenty-Second Annual Joint Conference of the IEEE Computer and Communications*. IEEE Societies, vol. 3. IEEE, 2003, pp. 1734–1743.
- [14] J. Bruck, J. Gao, and A. A. Jiang, "Localization and routing in sensor networks by local angle information," in *Proceedings of the 6th ACM international symposium on Mobile ad hoc networking and computing*. ACM, 2005, pp. 181–192.
- [15] Z. Zhong and T. He, "Achieving range-free localization beyond connectivity," in *Proceedings of the 7th ACM Conference on Embedded Networked Sensor Systems*. ACM, 2009, pp. 281–294.
- [16] D. Niculescu and B. Nath, "Dv based positioning in ad hoc networks," *Telecommunication Systems*, vol. 22, no. 1-4, pp. 267–280, 2003.
- [17] T. He, C. Huang, B. M. Blum, J. A. Stankovic, and T. Abdelzaher, "Range-free localization schemes for large scale sensor networks," in *Proceedings of the 9th annual international conference on Mobile computing and networking*. ACM, 2003, pp. 81–95.
- [18] M. Li and Y. Liu, "Rendered path: range-free localization in anisotropic sensor networks with holes," in *Proceedings of the 13th annual ACM international conference on Mobile computing and networking*. ACM, 2007, pp. 51–62.
- [19] C. Liu, K. Wu, and T. He, "Sensor localization with ring overlapping based on comparison of received signal strength indicator," in *Mobile Ad-hoc and Sensor Systems, 2004 IEEE International Conference on*. IEEE, 2004, pp. 516–518.
- [20] G. Wu, S. Wang, B. Wang, Y. Dong, and S. Yan, "A novel range-free localization based on regulated neighborhood distance for wireless ad hoc and sensor networks," *Computer Networks*, 2012.
- [21] F. Potorti, A. Corucci, P. Nepa, F. Furfari, P. Barsocchi, and A. Buffi, "Accuracy limits of in-room localisation using rssi," in *Antennas and Propagation Society International Symposium, 2009. APSURSI'09. IEEE*. IEEE, 2009, pp. 1–4.
- [22] A. Malekpour, T. Ling, and W. Lim, "Location determination using radio frequency rssi and deterministic algorithm," in *Communication Networks and Services Research Conference, 2008. CNSR 2008. 6th Annual*. IEEE, 2008, pp. 488–495.
- [23] H. Lee, A. Cerpa, and P. Levis, "Improving wireless simulation through noise modeling," in *Information Processing in Sensor Networks, 2007. IPSN 2007. 6th International Symposium on*. IEEE, 2007, pp. 21–30.
- [24] Z. Zhong, T. Zhu, D. Wang, and T. He, "Tracking with unreliable node sequences," in *INFOCOM 2009, IEEE*. IEEE, 2009, pp. 1215–1223.
- [25] C. Papamanthou, F. P. Preparata, and R. Tamassia, "Algorithms for location estimation based on rssi sampling," in *Algorithmic Aspects of Wireless Sensor Networks*. Springer, 2008, pp. 72–86.
- [26] Q. Zhang, G. Sobelman, and T. He, "Gradient-driven target acquisition in mobile wireless sensor networks," in *Mobile Ad-hoc and Sensor Networks*. Springer, 2006, pp. 365–376.
- [27] C. V. Durell, *Modern geometry: the straight line and circle*. Macmillan and Company, 1920.
- [28] Y. Shang, W. Ruml, Y. Zhang, and M. P. Fromherz, "Localization from mere connectivity," in *Proceedings of the 4th ACM international symposium on Mobile ad hoc networking & computing*. ACM, 2003, pp. 201–212.
- [29] A. K. Paul and T. Sato, "Detour path angular information based range-free localization in wireless sensor network," *Journal of Sensor and Actuator Networks*, vol. 2, no. 1, pp. 25–46, 2013.
- [30] N. M. Drawil, H. M. Amar, and O. A. Basir, "Gps localization accuracy classification: A context-based approach," 2013.
- [31] Q. Zhang, Y. Gu, L. Gu, Q. Cao, and T. He, "Collaborative scheduling in highly dynamic environments using error inference," in *Mobile Ad-hoc and Sensor Networks (MSN), 2011 Seventh International Conference on*. IEEE, 2011, pp. 105–114.
- [32] J. Pan, L. Cai, Y. T. Hou, Y. Shi, and S. X. Shen, "Optimal base-station locations in two-tiered wireless sensor networks," *Mobile Computing, IEEE Transactions on*, vol. 4, no. 5, pp. 458–473, 2005.
- [33] L. Ding, X. Gao, W. Wu, W. Lee, X. Zhu, and D.-Z. Du, "Distributed construction of connected dominating sets with minimum routing cost in wireless networks," in *Distributed Computing Systems (ICDCS)*. IEEE, 2010, pp. 448–457.